Hindawi
International Journal of Antennas and Propagation
Volume 2023, Article ID 2758371, 12 pages
https://doi.org/10.1155/2023/2758371

Research Article

Design of a Novel Superwideband Dual Port Antenna with Second-Order Hilbert Branches and a Modified T-Decoupling Structure

Jingchang Nan, Junru Pan, Xinxin Han, and Yifei Wang

The Key Laboratory of Wireless Communication Circuit System and Artificial Intelligence, School of Electronics and Information Engineering, Liaoning Technical University, Huludao, Liaoning 125105, China

Correspondence should be addressed to Junru Pan; 2546342989@qq.com

Received 3 December 2022; Revised 3 February 2023; Accepted 5 April 2023; Published 22 April 2023

Academic Editor: Jun Xiao

A novel super wideband (SWB) dual port antenna with second-order Hilbert branches and a modified T-decoupling structure is proposed. The overall size of the antenna is only 32 mm × 26 mm × 1 mm. The SWB antenna front comprises a "house" shaped radiating patch and a trapezoidal-shaped microstrip line. Two SWB antenna units are placed symmetrically on FR4 dielectric substrate to form the SWB-MIMO (multiple-in multiple-out) antenna. Two second-order Hilbert branches expand the wideband of the SWB-MIMO antenna. The antenna decoupling is mainly achieved by loading a fence-like "T" decoupling structure on the ground plane. The antenna is also miniaturized and isolated by adjusting the distance between the radiating patches of the units. The simulations and measurements show that the SWB-MIMO antenna operates in the frequency band of 1.98-30.8 GHz (175.84% relative bandwidth). The bandwidth dimensional ratio (BDR) (BDR is a measure of the compactness of the antenna, the higher the BDR, the better the compactness of the antenna, and the wider the working bandwidth of the antenna.) is 14653.33. The overall isolation is below −16.4 dB, and the important part (8.5–24.1 GHz) is below −20 dB. The envelope correlation coefficient (ECC) is less than 0.03, and the radiation characteristics are excellent.

1. Introduction

With today's advances in wireless communications technology and other related fields, the need for significantly higher data rates in next-generation wireless systems is challenging for the communications systems industry. In traditional single-input single-output (SISO) technology, more thought has been given to reducing or avoiding multipath fading, and thus increasing channel capacity. Still, this has yet to be able to break through the capacity limit, which can be improved by MIMO technology [1–3]. The term "ultrawideband" was first proposed by the US Department of Defense in 1989. In 2002, the FCC defined 3.1~10.6 GHz as the civilian ultrawideband band and defined the signal with a relative bandwidth greater than 20% at −10 dB as an ultrawideband signal [4–6]. UWB (ultra wideband) antenna bandwidth of the highest cutoff frequency and the lowest cutoff frequency ratio of more than 10 : 1 can be seen as super bandwidth (SWB) antenna. Moreover, the SWB antenna band covers the UWB antenna band range for long-range and short-range communications. The SWB antenna covers long and short-range communications within the UWB antenna band and has a much wider bandwidth [7–9]. The compactness of the antenna structure and the wide bandwidth range are two decisive factors for the performance and efficiency of the antenna. Simultaneously, the coupling between them becomes a problem that cannot be ignored with the increased number of antenna units. The coupling effect will make the performance of the communication system suffer, so it is vital to improving the antenna isolation. Improving the isolation between antenna units is also miniaturization, so miniaturization of antennas is essential. Taking the superbandwidth of the antenna as a premise, ensuring the miniaturization of the antenna while reducing the mutual coupling between multiple antenna units is a worthy challenge in antenna design. Therefore, the study of miniaturized SWB-MIMO antennas is necessary.

In the past few years, the antenna spectrum research direction has increased from UHF (300MHz-3 GHz) to microwave, millimeter wave, etc. Looking far into the future, the spectrum range above 6 GHz and millimeter wave band are the focus of research and development. In literature [10], a 27 mm × 47 mm × 1.6 mm UWB-MIMO antenna is proposed. This antenna with a short inverted "Y" cutoff line loaded on the ground plate surface so that the isolation of the antenna in the whole UWB frequency range is less than −17 dB. In literature [11], a 20 mm × 47 mm × 1.6 mm SWB-MIMO antenna is proposed. And the SWB-MIMO antenna is placed symmetrically with the middle of the two ship-shaped monopole antennas vacant for a distance. And the isolation is less than −16 dB to achieve an operating bandwidth of 2.97~19.82 GHz. In literature [12], a 30 mm × 41 mm × 1.59 mm UWB-MIMO antenna is proposed to achieve an operating bandwidth of 2.2~11 GHz. The second iteration of the Hilbert fractal slot is continued to be etched on top of the ground plate with two circles removed to enhance the isolation to improve the isolation. In addition, the addition of parasitic cells and neutralization lines are common methods to improve the isolation of the antenna. A 90 mm × 45 mm × 2 mm SWB-MIMO antenna is proposed in literature [13], which places low-profile coplanar waveguide-fed elliptical patches in parallel and eventually achieves a bandwidth band of 2.2473 to 30 GHz with a relative bandwidth of 172.12%. Although several antennas mentioned in the literature have better operating performance in the passband, their sizes are large. It is worthwhile to carefully study how to balance size, bandwidth, and isolation.

This article proposes a novel super wideband dual port antenna with second-order Hilbert branches and a modified T-decoupling structure. The radiating patch is a "house" shaped by combining trapezoidal and rectangular shapes. Second-order Hilbert branches are introduced to achieve the superwideband; a fence-like "T" decoupling structure is presented on the ground plane to improve the antenna isolation. The final size of the antenna is only 32 mm × 26 mm × 1 mm, which is very compact, and the isolation is below −16.4 dB in the operating bandwidth of 1.98~30.8 GHz, the bandwidth ratio is 15.6 : 1, the bandwidth dimensional ratio (BDR) is 14653.33, and the envelope correlation coefficient (ECC) is below 0.03. The actual test results are consistent with the simulation results. It shows that the antenna has good gain and radiation characteristics and can be well used in miniaturized SWB-MIMO systems.

2. SWB-MIMO Antenna Design and Analysis

2.1. Design of SWB Antenna. A miniaturized SWB antenna designed in this article is only 16 mm × 26 mm in size and is fed by a trapezoidal microstrip line structure with a port impedance of 50 Ω. The antenna is printed on a 1 mm thick FR4 dielectric substrate with a dielectric constant of 4.4 and a loss angle tangent of 0.02. The evolution of the antenna unit is shown in Figure 1.

Figure 2 shows the S_{11} results corresponding to different structures during the evolution of the antenna unit. The figure shows that the S_{11} part of the rectangular patch in antenna 1 is above −10 dB. It does not meet the working requirements of the antenna. Antenna 2, after cutting the angle of the radiation patch and stepping the feed line, the S_{11} is effectively improved, and most of the bandwidth is below −10 dB. The bandwidth at high frequency is widened to 26.3 GHz. Antenna 3, S_{11} is greater than −10 dB at 16 GHz. It does not meet the working requirements of the antenna. Antenna 4 optimizes the structure of the radiation patch and feed line interface. The overall working band reaches the antenna requirements. The final working bandwidth is expanded to 1.2~23.3 GHz. It reaches the condition that the ratio of the highest cutoff frequency to the lowest cutoff frequency in the SWB working band is greater than 10 : 1. We can see that improving the antenna radiation patch structure plays a particular role in expanding the antenna bandwidth through the S_{11} data. The antenna radiation patch is a gradient structure, which dramatically expands the working bandwidth of the antenna.

In order to investigate the effects of digging out the short triangular edge and inverted trapezoidal height on the antenna performance, the W_t and L_f sizes are optimized while keeping the other parameters constant. Figures 3(a) and 3(b) show the S_{11} results for optimizing W_t and L_f. From Fig. 3(a), it can be seen that the amplitudes are similar for different lengths of W_t. The results of S_{11} are optimized when $W_t = 0.7$ mm. From Figure 3(b), it can be seen that the S_{11} results are optimal when $L_f = 1.1$ mm. With the increase in frequency, the operating band of the antenna also has a small expansion.

2.2. Design of SWB-MIMO Antenna. SWB-MIMO antenna is a special ultrawideband MIMO antenna. The SWB-MIMO wideband concludes the UWB-MIMO antenna wideband. SWB-MIMO antenna operating band contains the frequency band of the UWB-MIMO antenna. It is challenging to design an antenna that needs all excellent performance. The antenna structure requirements are very high. Using a graduated structure of the radiating patch and adding a second-order Hilbert branch can increase the current flow path, and thus extend the operating bandwidth of the antenna.

The antenna structure designed and the specific dimensions of the antenna area are marked in Figure 4, with dimensions of 32 mm × 26 mm × 1 mm. The radiation patches of the antenna are made up of a trapezoidal structure, a rectangular structure, and a smaller inverted trapezoidal structure, respectively. Two trapezoids are placed on the upper and lower sides of the rectangle to increase the radiation patch area. At the same time, it enhances the radiation performance of the antenna. Introducing two second-order Hilbert branches in the middle of the two units greatly expands the antenna's bandwidth at high frequencies. Figure 5 shows the S_{11} results of the SWB-MIMO antenna without and with the number of second-order Hilbert branches.

The introduction of parasitic branches can increase the resonance point, using a similar method of interleaved

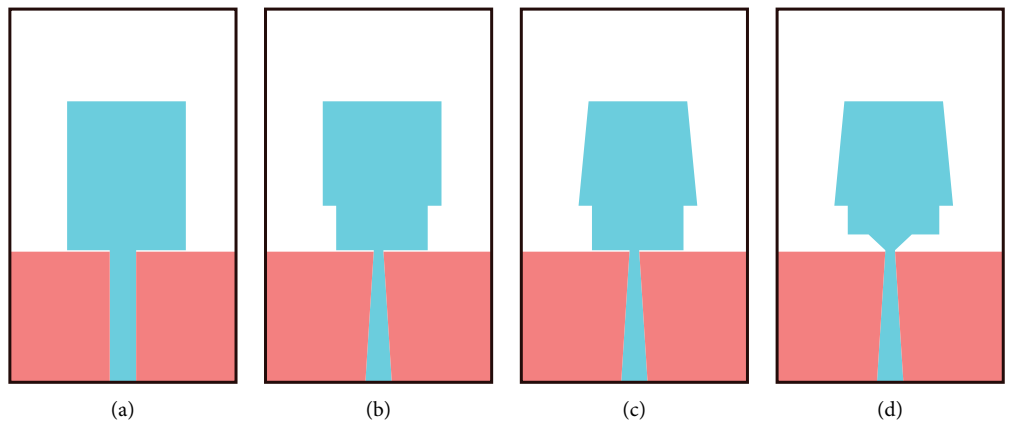

Figure 1: Evolution of the antenna unit. (a) Antenna 1. (b) Antenna 2. (c) Antenna 3. (d) Antenna 4.

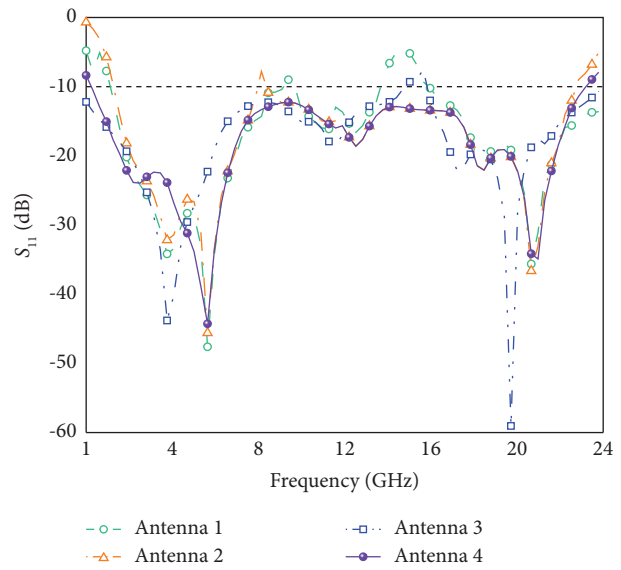

Figure 2: Different S_{11} corresponding to different patch.

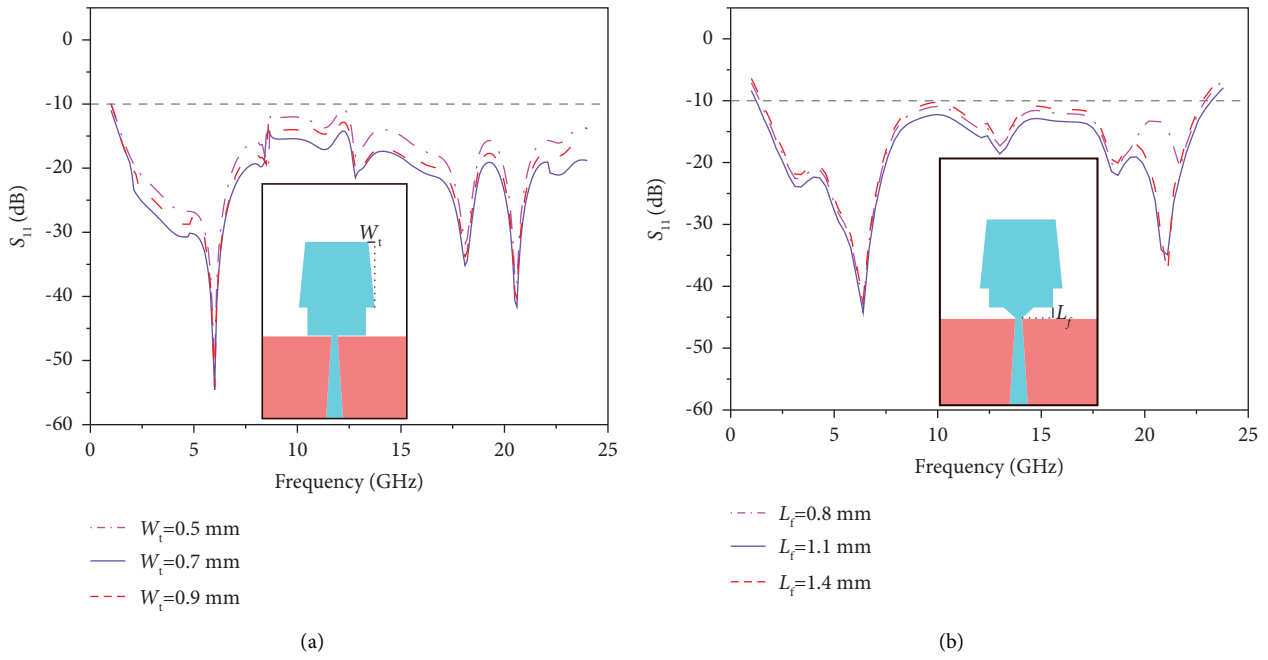

Figure 3: S_{11} simulation results of different long side values. (a) W_t. (b) L_f.

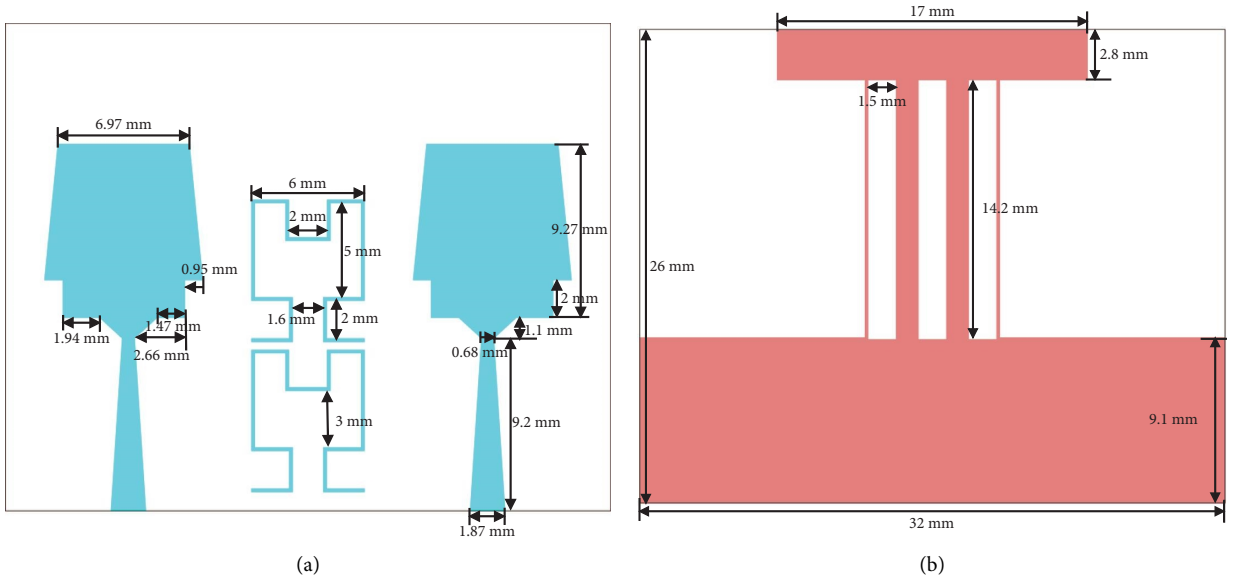

Figure 4: SWB-MIMO antenna structure. (a) Front. (b) Back.

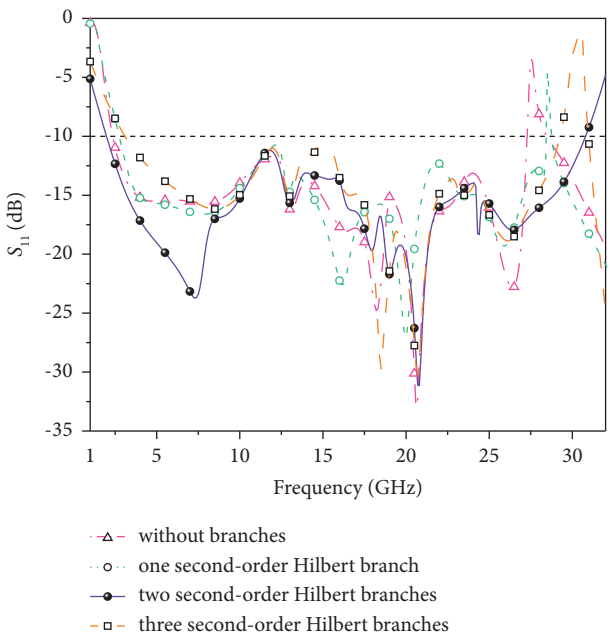

Figure 5: S_{11} results in the addition of the branch and for different numbers of branches.

tuning so that it is located near the original resonant frequency to broaden the operating band of the antenna, generally adding 2~5 parasitic branches. The patch size is different, so its resonant frequency is also different. The disadvantage of using parasitic branches is that they increase the size of the antenna. Most parasitic branches with an asymmetrical structure result in poor stability of the radiation pattern in the operating band of the antenna. To solve the possible impact of introducing parasitic dendrites on the original antenna, the proposed SWB-MIMO antenna places the second-order Hilbert dendrites in the middle of the two antenna units without increasing the original physical size of the antenna. The second-order Hilbert dendrites are symmetrical about the center line of the dielectric substrate, which does not seriously impact the antenna's omnidirectional radiation performance.

The S_{11} results in the addition of the branch and for different numbers of branches are shown in Figure 5. As seen from the figure, the bandwidth of 2.3–27.2 GHz satisfies the SWB-MIMO antenna without the introduction of the branch. After introducing the second-order Hilbert branch in the middle of the antenna unit, its bandwidth expands to 28.72 GHz at high frequencies. This result indicates that the branch is useful for expanding the bandwidth. Continuing to add the same second-order Hilbert branch, the bandwidth of the SWB-MIMO antenna is expanded to 1.98-30.8 GHz. The operating bandwidth band is reduced when the third second-order Hilbert branch is added. Therefore, when two second-order Hilbert branches are added, the operating bandwidth of the antenna is expanded to the broadest possible range.

A 50 Ω trapezoidal-shaped microstrip feed line with a port width of 1.87 mm is used, and the two antenna units are placed symmetrically on the dielectric substrate according to the relevant values of the materials and dimensions used and the microstrip line calculation formula. A fence-like "T" decoupling structure is added to the basic rectangular ground plate. The distance between the two antenna units is adjusted to reduce the mutual coupling between the antenna units, resulting in a miniaturized MIMO antenna with SWB characteristics.

2.3. Antenna Decoupling Structure Design and Optimization Analysis. While maintaining the compactness of the miniaturized SWB-MIMO antenna, it is difficult further to improve the isolation and performance of the antenna. The principle of the decoupling structure is to change the antenna current path, and the decoupling structure blocks the current

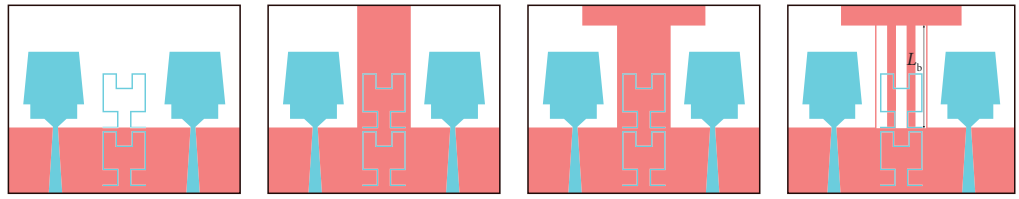

Figure 6: Evolution of the SWB-MIMO antenna decoupling structure. (a) Antenna 5. (b) Antenna 6. (c) Antenna 7. (d) Antenna 8.

to limit the current to one end of the antenna as much as possible to improve the isolation of the antenna. [14–16].

To achieve the required antenna isolation in the entire frequency band without increasing the antenna's physical size, a simple fence-like "T" decoupling structure is proposed in this article. This decoupling structure reduces the antenna's overall isolation to −16.4 dB, and the isolation is below −20 dB at 8.5~24.1 GHz band. The evolution of the decoupling structure is shown in Figure 6.

Firstly, the "I" type decoupling structure is introduced on the rectangular ground plate, which can act as a reflector to block the current flow between the antenna units and use its structure to disperse the current, which plays a significant role in improving the isolation. The "I" decoupling structure is kept in the same position, and the "T" decoupling structure is obtained by further improving the "I" decoupling structure and etching several rectangular slot slits with the etched. The etched slot slits are a slow wave structure that reduces the signal wavelength and increases the effective electrical length between the antenna units. Finally, after optimizing the size, number, and position of the etched rectangular slits, three rectangular slits are etched into the vertical part of the "T" decoupling structure to form a fence, which has a more pronounced effect on current dispersion and achieves improved isolation in the operating frequency band. Figure 7 shows S_{21} in the evolution of the SWB-MIMO antenna structure, from which the isolation degree at the middle band of antenna 5 is greater than −15 dB, which does not meet the requirements; for antenna 6, the "I" type decoupling structure is improved compared to antenna 5; the "T" type decoupling structure of antenna 7 makes the SWB-MIMO antenna more isolated. The "T" decoupling structure of antenna 7 makes the SWB-MIMO antenna meet the requirements from 5 to 27.6 GHz, but the isolation between low and high frequencies is still high; the fence-like "T" decoupling structure of antenna 8 meets the requirements of the SWB-MIMO antenna, but also expands the operating bandwidth of the SWB-MIMO antenna. MIMO antenna's operating bandwidth is extended to 1.98~30.8 GHz.

After several simulations, three rectangular slits are etched on the "T" decoupling structure, the position of the rectangular slits is adjusted, and the value of the length of the rectangular slits L_b is continuously optimized when the value of L_b is different. The corresponding isolation degree S_{21} also changes. The optimization result is shown in Figure 8. When $L_b = 14.2$ mm, the maximum isolation of the whole working band of the antenna is reduced to −16.4 dB, which shows

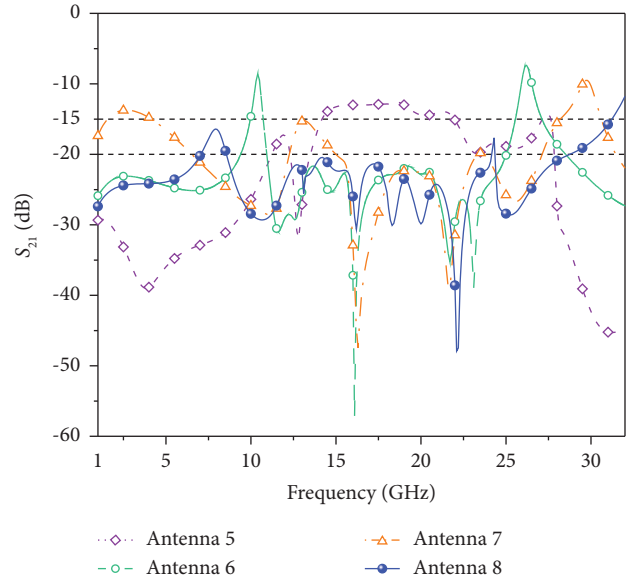

Figure 7: S_{21} corresponding to the evolution of the SWB-MIMO antenna structure.

that the fence-like "T" decoupling structure plays a significant role in the reduction of isolation.

The design of the fence-like "T" decoupling structure can increase the current path and change the current path while limiting the current in its structure. To a certain extent, it reduces the current interchange between the excitation and the nonexcitation end, reduces the coupling between the two units, and will not generate additional radiation. At the same time, the "T" decoupling structure and the nonexcitation end antenna unit to the excitation end antenna will also produce coupling. These coupling effects cancel each other, reducing the isolation between the two units of the antenna and meeting the requirements of the antenna isolation but also ensuring the excellent performance of the antenna.

2.4. Antenna Surface Current Distribution. Figure 9 shows the surface current distribution of the antenna at the center of the operating bandwidth of 16 GHz; during the evolution of this SWB-MIMO antenna ground plate structure. Different decoupling structures have different effects on antenna isolation and different effects on the current hindrance. From Figure 9(a), the rectangular ground plate couples a large amount of current to port 2 with the

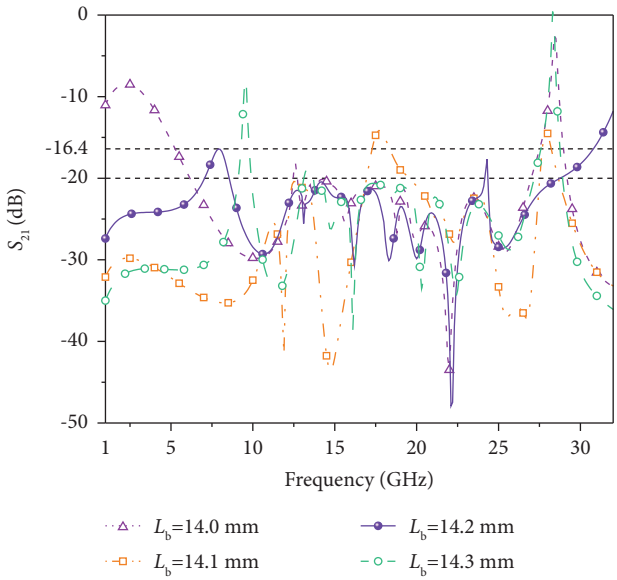

FIGURE 8: S_{21} results for different values of L_b.

excitation of port 1 and has little effect on current dispersion. In Figure 9(c), a small amount of current is observed on the surface of the antenna unit at the nonexcited end; in Figure 9(d), only a tiny scattered current is observed on the surface of the antenna unit at the nonexcited section. Therefore, it is also verified that the isolation of the SWB-MIMO antenna can be effectively improved by the fence-like "T" decoupling structure.

In Figure 10, the current distribution at 2 GHz, 10 GHz, 20 GHz, and 30 GHz are taken to observe the degree of antenna isolation. The current distribution of the antenna at these four frequency points and the decoupling structure of the antenna effectively blocks most of the current, thus reducing the coupling between the two units and making the overall isolation of the antenna lower.

2.5. Bandwidth Dimensional Ratio (BDR). The bandwidth dimensional ratio (BDR) is a measure of the compactness of an antenna and a measure of the super bandwidth. The higher the BDR, the better the design of the antenna, the more compact the antenna, and the wider the operating bandwidth.

$$BDR = \frac{\%Bandwidth}{\lambda length \times \lambda width}, \quad (1)$$

where %*B*andwidth is the relative bandwidth, λlength is the length of the electrical dimension, and λwidth is the width of the electrical dimension. The electrical dimension of this antenna is $0.12\lambda \times 0.1\lambda$ (λ is the wavelength corresponding to the lowest resonant frequency in the operating bandwidth of the antenna), and the relative bandwidth of the antenna is 175.84%. The goal of the design is to obtain a miniaturized SWB-MIMO antenna. Therefore, the BDR of the SWB-MIMO antenna proposed in this article is calculated to be 14653.33 according to equation (1), which indicates that this antenna is sufficiently compact.

3. Results and Discussion

In order to test the performance of the proposed miniaturized SWB-MIMO antenna, the antenna was modeled, exported by CAD software, and machined. The SMA connector was soldered, and the cable was connected to test *S*-parameters and other indicators. The physical drawing is shown in Figure 11.

3.1. S-Parameters. *S* parameter is one of the important indexes to reflect the antenna's performance. Figure 12 shows the simulated and measured data results of S_{11} and S_{21}, from which we can see that the SWB-MIMO antenna in 1.98~30.8 GHz S_{11} is less than −10 dB, and S_{21} is less than −16.4 dB in its working bandwidth. The simulated and measured results may have errors within a reasonable range, but the main performance of the antenna does not change significantly as shown in Figure 12, which shows that the SWB-MIMO antenna has good isolation and other performance.

3.2. Radiation Characteristics. Figure 13 shows the antenna's simulated and measured two-dimensional radiation pattern in the far field *E* and *H* planes at 2 GHz, 10 GHz, 15 GHz, 20 GHz, 25 GHz, and 30 GHz. Some degradation of the radiation pattern may occur during the actual measurements, which may be due to material loss during processing and actual measurements. From the overall view of Figure 13, the radiation effect is relatively stable.

The peak gain of the antenna is one of the key indicators to measure the stability of the antenna. As seen in Figure 14, the simulation of peak gain is more consistent with the actual measurement, and the peak gain has small fluctuations between 4 GHz and 6 GHz, but all remain smooth, indicating that the antenna has stable performance and good radiation performance.

3.3. ECC. For MIMO antennas, the enveloped correlation coefficient can illustrate the correlation between the two units of the antenna. The smaller the value of ECC means that the higher the independence between the antenna units, the ideal value of ECC is 0. However, the value of ECC is less than 0.5 in practice. The ECC of a two-port MIMO antenna can be calculated according to equation (2).

$$ECC = \frac{\left|S_{11}^{*}S_{12} + S_{21}^{*}S_{22}\right|^2}{\left(1 - \left|S_{11}\right|^2 - \left|S_{21}\right|^2\right)\left(1 - \left|S_{22}\right|^2 - \left|S_{12}\right|^2\right)}, \quad (2)$$

where S_{11}^{*} is the conjugate value of S_{21}^{*}. The comparison between the simulated and measured ECC of the SWB-MIMO antenna designed in this article is shown in Figure 15. This data shows that this antenna's ECC is less than 0.03 in its operating band. It indicates that the antenna

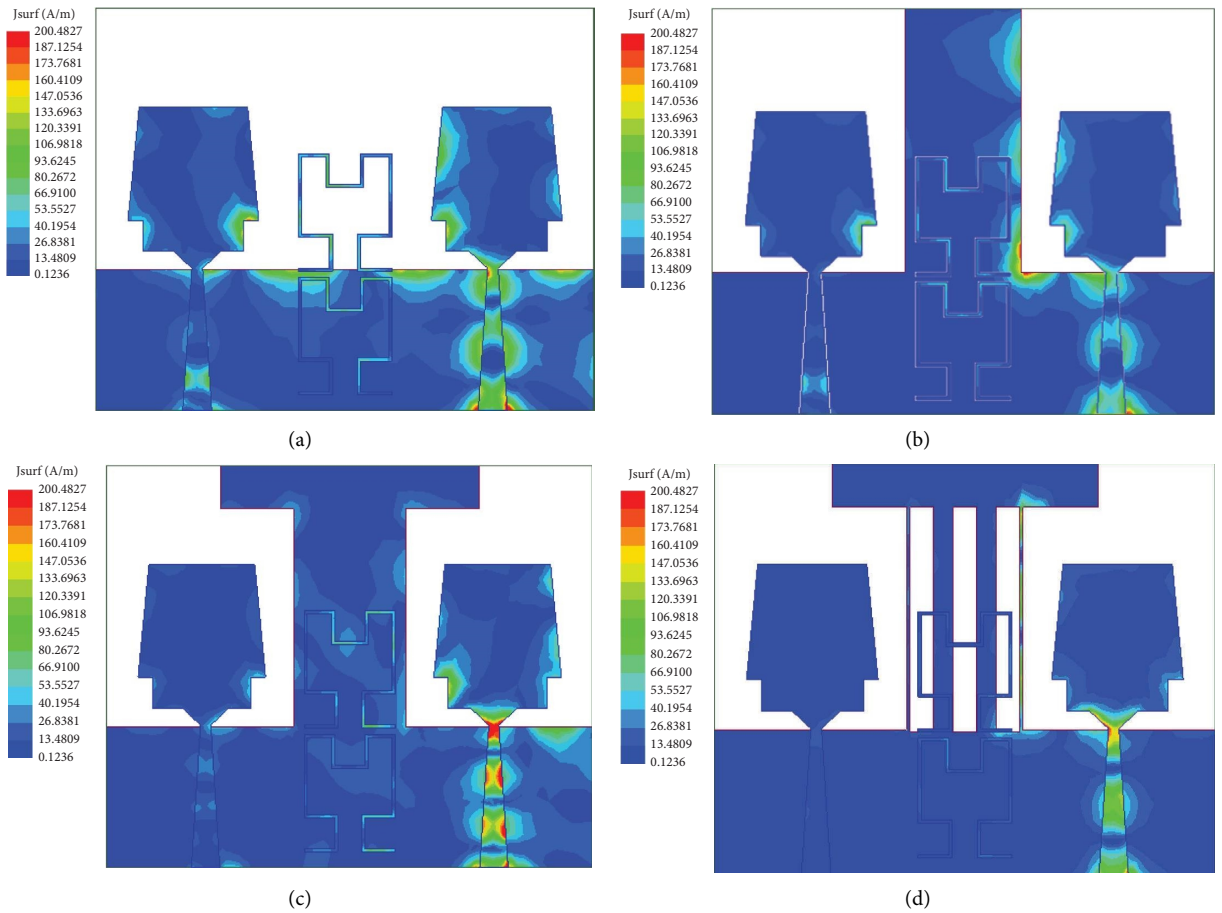

Figure 9: Current distribution of SWB-MIMO antennas at 16 GHz for different decoupling structures. (a) Antenna 5. (b) Antenna 6. (c) Antenna 7. (d) Antenna 8.

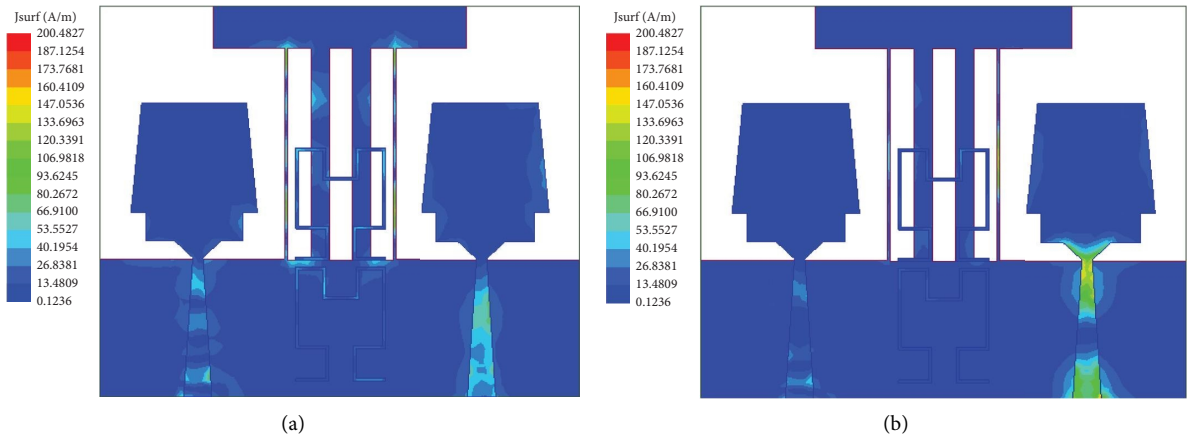

Figure 10: Continued.

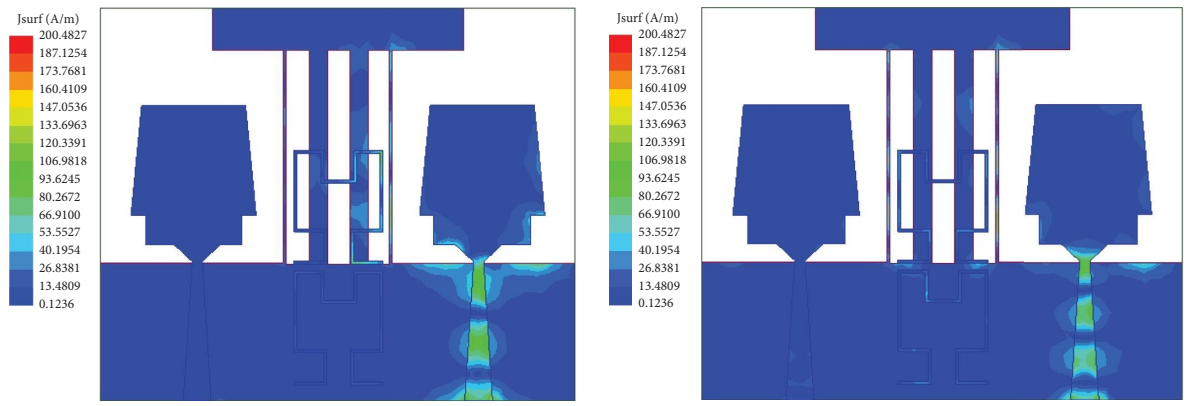

(c) (d)

Figure 10: SWB-MIMO current distribution at different frequency points. (a) 2 GHz. (b) 10 GHz. (c) 20 GHz. (d) 30 GHz.

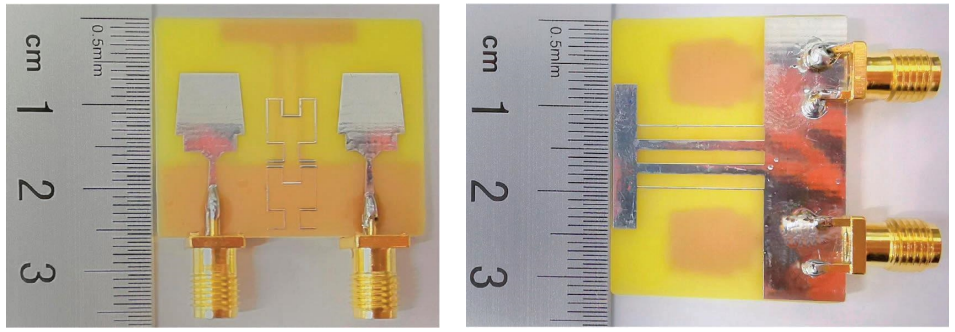

(a) (b)

Figure 11: Physical view of the antenna. (a) Top. (b) Bottom.

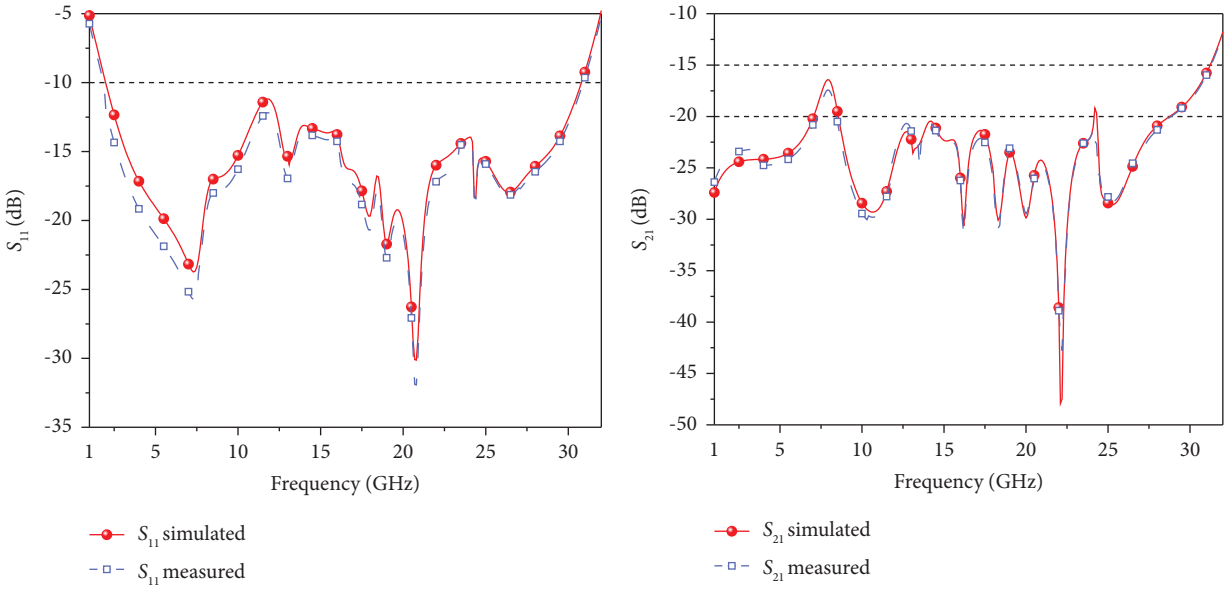

(a) (b)

Figure 12: Simulation and measurement of S_{11} and S_{21}. (a) S_{11} simulation and measurement. (b) S_{21} simulation and measurement.

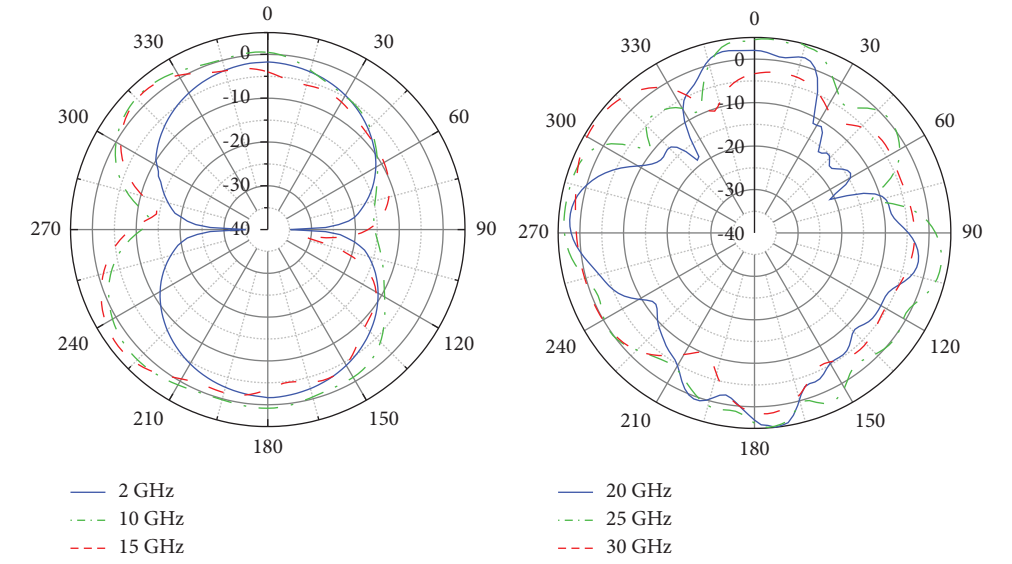

(a)

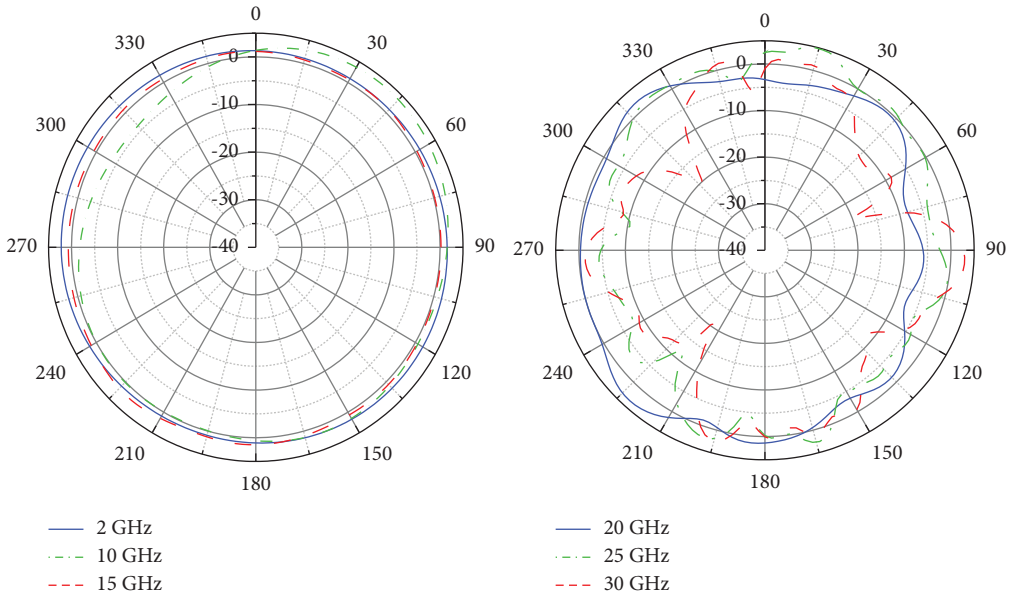

(b)

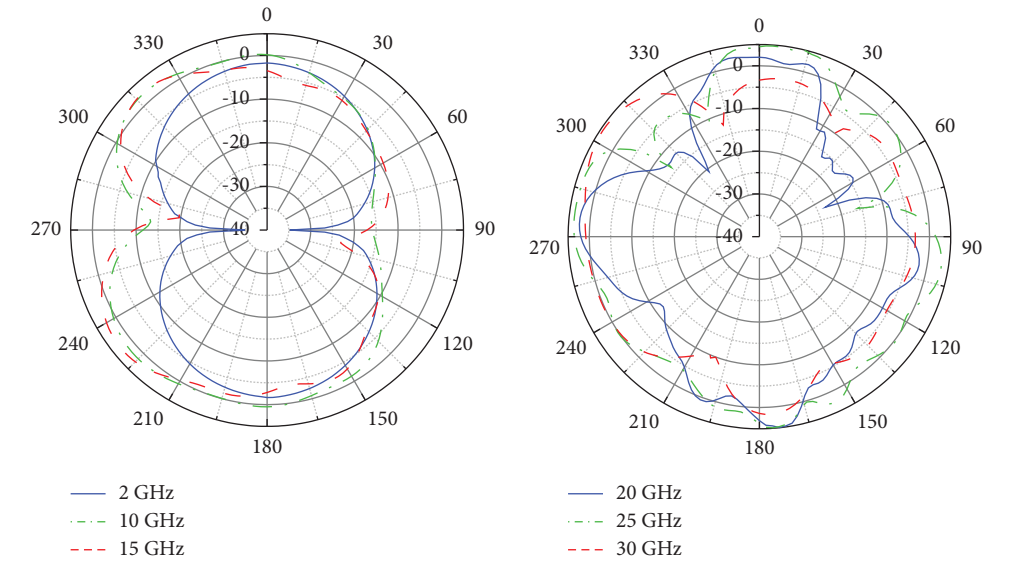

(c)

Figure 13: Continued.

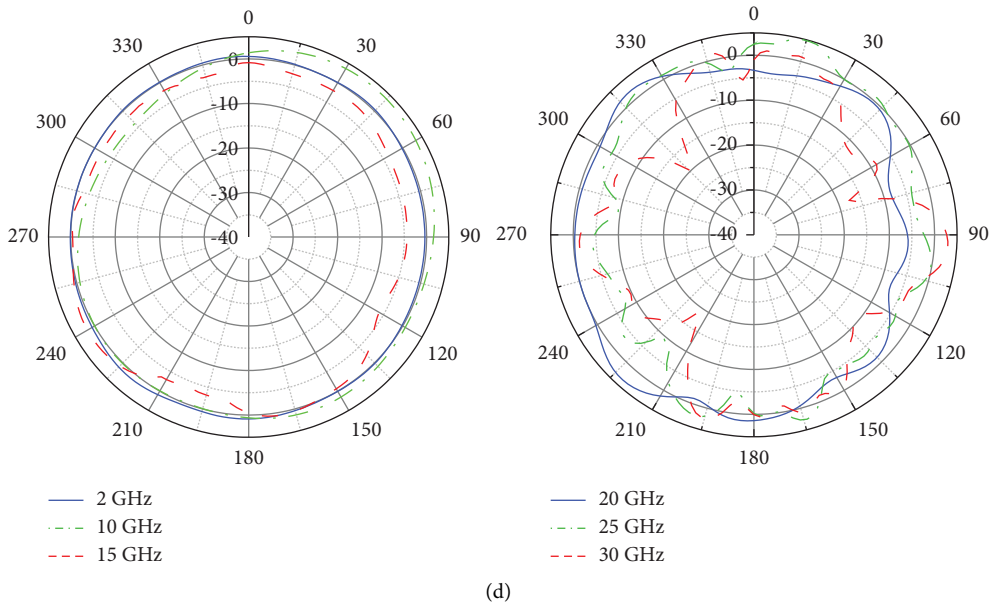

Figure 13: *E*. *H*-plane simulation and real measurement results. (a) *E*-surface simulation results. (b) *H*-surface simulation results. (c) *E*-surface real measurements results. (d) *H*-surface real measurements results.

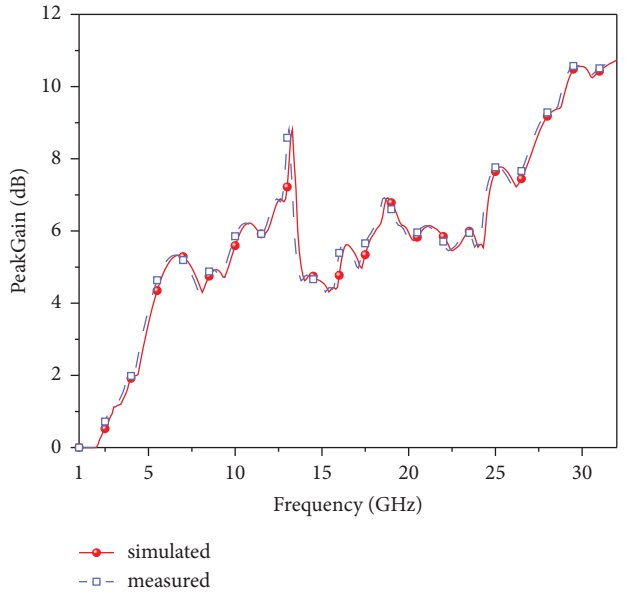

Figure 14: Peak gain of the antenna.

has strong independence between each unit, fully reflecting the good performance of this SWB-MIMO antenna.

Table 1 shows the performance parameters of the miniaturized SWB-MIMO antenna designed in this article compared with those in the published literature. As seen from the table, compared with other SWB-MIMO antennas, although both have a wider operating bandwidth, the proposed antenna is smaller and more compact. It has a larger relative bandwidth, which better balances the relationship between antenna size and operating bandwidth, and the antenna structure has the advantage of being smaller and more compact.

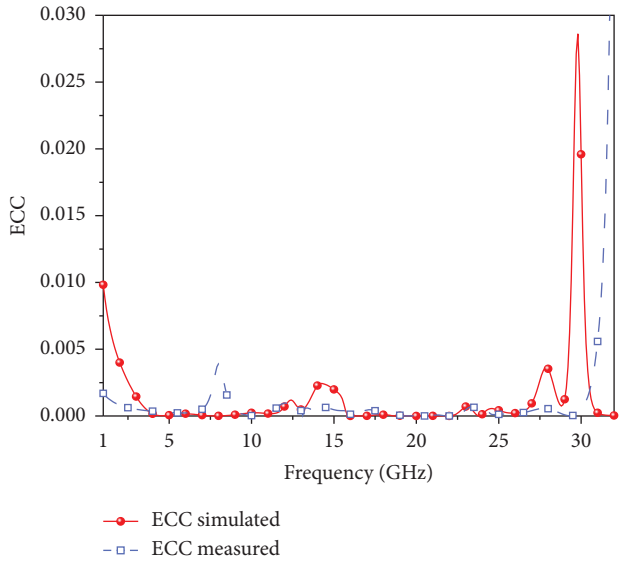

Figure 15: ECC simulation and real testing.

Table 1: Performance of the proposed SWB-MIMO antenna and referenced antennas.

Refer-ence	No of elements	Dimension (mm^3)	Bandwidth (GHz)	Relative bandwidth (%)	BDR	Isolation (dB)	ECC
[2]	2	$20 \times 47 \times 1.6$	2.97~19.82	148.1	1575.53	<-16	—
[5]	2	$56 \times 50 \times 1.67$	4~40	163.64	442.27	<-20	<0.018
[6]	4	$52 \times 52 \times 1.6$	1.25~40	187.88	4260.32	<-18	<0.09
[16]	2	$40 \times 70 \times 1.6$	2~20	163.63	3164.72	<-15	<0.018
This article	2	$32 \times 26 \times 1$	1.98~30.8	175.84	14653.33	<-16.4	<0.03

4. Conclusions

In this article, a novel SWB dual port antenna with second-order Hilbert branches and a modified T-decoupling structure is designed. The antenna size is 32 mm × 26 mm × 1 mm, the BDR is 14653.33, and the operating band is 1.98~30.8 GHz, covering all types of UWB applications and higher frequency bands such as Ku and K. The antenna below −16.4 dB meets the requirements of the SWB-MIMO antenna, and the ECC < 0.03 indicate that the antenna has good diversity performance and can be widely used in the wireless communication system.

Data Availability

All data generated or analyzed during this study are included within the article.

Conflicts of Interest

The authors declare that they have no conflicts of interest.

Acknowledgments

This study was supported by the National Natural Science Foundation of China (61971210).

References

[1] S. Singhal, "Feather-shaped super wideband MIMO antenna," *International Journal of Microwave and Wireless Technologies*, vol. 13, pp. 94–102, 2021.

[2] L. Wu, Y. Xia, X. Cao, and Z. Xu, "A miniaturized UWB--MIMO antenna with quadruple band-notched characteristics," *International Journal of Microwave and Wireless Technologies*, vol. 10, pp. 948–955, 2018.

[3] H. Ullah, S. U. Rahman, Q. Cao, I. Khan, and H. Ullah, "Design of SWB MIMO antenna with extremely wideband isolation," *Electronics*, vol. 9, no. 1, p. 194, 2020.

[4] M. K. Abdelazeez, N. M. Awad, and A. S. Abbas, "UWB antenna with super bandwidth," in *Proceedings of the 2016 IEEE International Symposium on Antennas and Propagation (APSURSI)*, IEEE, Fajardo, PR, USA, June 2016.

[5] B. Premalatha, G. Srikanth, and G. Abhilash, "Design and analysis of multi band notched MIMO antenna for portable UWB applications," *Wireless Personal Communications*, vol. 118, pp. 1697–1708, 2021.

[6] C. Yu, S. Yang, Y. Chen et al., "A super-wideband and high isolation MIMO antenna system using a windmill-shaped decoupling structure," *IEEE Access*, vol. 8, Article ID 115767, 2020.

[7] A. Bhattacharya, B. Roy, and A. K. Bhattacharjee, "Compact, isolation enhanced, band-notched SWB–MIMO antenna suited for wireless personal communications," *Wireless Personal Communications*, vol. 116, no. 3, pp. 1575–1592, 2021.

[8] D. Kumar Raheja, S. Kumar, B. Kumar Kanaujia, S. Kumar Palaniswamy, R. Rao Thipparaju, and M. Kanagasabai, "Truncated elliptical Self-Complementary antenna with Quad-Band notches for SWB MIMO systems," *AEU - International Journal of Electronics and Communications*, vol. 131, Article ID 153608, 2021.

[9] P. Gireesh, P. S. Kumar, K. Malathi, I. Khanra, A. Agarwal, and K. Sivakumar, "Design and analysis of dual port super WideBand antenna set for MIMO applications," *Journal of Physics: Conference Series*, vol. 1964, no. 6, 2021.

[10] M. S. Khan, M. F. Shafique, A. D. Capobianco, E. Autizi, and I. Shoaib, "Compact UWB-MIMO antenna array with a novel decoupling structure," in *Proceedings of the 2013 10th International Bhurban Conference on Applied Sciences and Technology (IBCAST)*, IEEE, Islamabad, Pakistan, January 2013.

[11] A. Gorai, A. Dasgupta, and R. Ghatak, "A compact quasi-self-complementary dual band notched UWB MIMO antenna with enhanced isolation using Hilbert fractal slot," *AEU - International Journal of Electronics and Communications*, vol. 94, pp. 36–41, 2018.

[12] M. A. I. Oni, S. H. Shehab, S. Hassan, and S. Dey, "Design and analysis of a low-profile, elliptical patch Super Wide Band (SWB) MIMO antenna," in *Proceedings of the 2015 International Conference on Advances in Electrical Engineering (ICAEE)*, IEEE, Dhaka, Bangladesh, December 2015.

[13] G. Saxena, V. Prajapati, V. Gupta, and S. Kumar, "High isolation with mushroom shaped EBG super wide band MIMO antenna," in *Proceedings of the 2021 International Conference on Advance Computing and Innovative Technologies in Engineering (ICACITE)*, IEEE, Greater Noida, India, March 2021.

[14] D. K. Raheja, S. Kumar, and B. K. Kanaujia, "Compact quasi-elliptical-self-complementaryfour-port super-wideband MIMO antenna with dual band elimination characteristics," *AEU - International Journal of Electronics and Communications*, vol. 114, Article ID 153001, 2020.

[15] M. Irshad Khan, M. I. Khattak, S. U. Rahman, A. B. Qazi, A. A. Telba, and A. Sebak, "Design and investigation of modern UWB-MIMO antenna with optimized isolation," *Micromachines*, vol. 11, no. 4, p. 432, 2020.

[16] W. Balani, M. Sarvagya, A. Samasgikar, T. Ali, and P. Kumar, "Design and analysis of super wideband antenna for microwave applications," *Sensors*, vol. 21, p. 477, 2021.